Characterization of the internal state of nitrogen-vacancy centerin diamond and second quantization formalism

C. I. Huerta[a], E. Urrutia-Bañuelos[a], M. R. Pedroza-Montero[a] and R. Riera[a,b,*]

[a]*Departamento de Investigación en Física, Universidad de Sonora, Apartado Postal 5-088, 83190 Hermosillo, Sonora, México.*

[b]*Centro de Investigación y Educación Superior CIES-UNEPROP. Blvd. José María Escribar 38 Col. Villa del Palmar, 83105 Hermosillo, Sonora, México.*

[*]*e-mail: rriera@cifus.uson.mx*

Received 21 January 2020; accepted 25 June 2020

In this paper a general study of nitrogen-vacancy center internal state in diamond is presented. This study is based on experimental and theoretical findings found in literature. First, a Hamiltonian model for center nitrogen-vacancy internal state is proposed in terms of a complete set of commuting observables (CSCO), which consist of angular momentum $\hat{L}$, spin momentum $\hat{S}$, total angular momentum $\hat{J} = \hat{L} + \hat{S}$, and spin momentum on z-direction $\hat{S}_z$. The second quantization formalism –in steady-state (conservative model)– is used. The creation and annihilation operators are used to described the steady spin-levels structure and in dynamic-state (non-conservative model) and can also describe the system dynamic between different spin-levels transitions. Finally, a discussion is presented about the application of this study in the photochromism phenomenon and solid-state quantum bit (qubit).

Keywords: NV Center; defect; photochromism; qubit.

PACS: 81.05.ug; 03.67.-a; 61.72.jn; 75.10.Jm; 75.10.Dg

DOI: https://doi.org/10.31349/RevMexFis.66.814

1. Introduction

The nitrogen-vacancy (NV) center is one of numerous point defects in diamond. It exhibits two electronic configurations: the neutral charged-state (NV^0) and the negatively charged-state (NV^-). The phenomenon called photochromism consists in the NV center interchange between two different charged-states by a possible mechanism involving nitrogen donors [1]. Electron spins at NV centers can be manipulated by applying a magnetic field, electric field, electromagnetic radiation (light), or a combination of them, resulting in a photoluminescent signal.

The photophysics of color NV centers in diamond have attracted interest during the last decade because of their possible application in quantum information processing, quantum optics, quantum metrology, nanotechnology, as biological and sub-diffraction limit imaging, to test of entanglement in quantum mechanics and nano-medicine (sensors) [2-5]. Currently, the technology tends to miniaturization, but it faces a problem: the integration techniques of circuits are not effective due to the quantum effects which become important in low dimensionality. Therefore, computational science has begun to research in quantum mechanics a new technological alternative with the aim to overcome the transistor technology.

The most promising systems are ions or atoms traps, which use their electronics states as representation of the quantum bit (qubit) states (*e.g.* ground and excited electronics states) [6]; quantum dots in which its confined electron spins are controlled by tunneling effect via electric field and each different electron-spin configuration is used as qubit state [7,8]; setting diverse magnetics polarizations as qubit states by using NMR to manipulate nuclear spins of one or lots of molecules, generally in liquid state [9,10]; superconducting loops with persistent current form a qubit by superposition of two macroscopic quantum states [11]; and the defects present in diamond, more precisely NV centers of which their electronic spins system are taken advantage, allowing to be initialized, manipulated, and measured (readout) by optical means [12].

At this moment, the available computing power is not enough. For this reason the Quantum Informatics become important. Apparently, the best candidate for solid-state qubit is the NV^- center in diamond since it works at room temperature, has long spin coherence time as well as the diamond lattice helps as an insulator for external magnetic effects because it is diamagnetic; in addition, thanks to its high Debye temperature, the vibrational modes of the lattice are not affecting the center because there is a low coupling between lattice phonons and center electrons [13,14]. In this paper a general study of internal state NV center in diamond is presented. From the second quantization formalism, –in steady-state (conservative model)– the creation and annihilation operators are used to describe the steady spin-levels structure and in dynamic-state (non-conservative model); these operators can also be used to describe different spin-level transitions. Finally, a discussion is presented about the applications of this study on different areas, especially in the photochromism phenomenon and solid-state qubit.

2. NV centers in diamond

The atomic configuration of NV center consists of two places that should be occupied with two carbon atoms but, instead, one carbon atom was replaced by a nitrogen atom and the other place is empty. In other words, there is a vacancy. The NV defect has point group C_{3v}, where the principal axis C_3 is along nitrogen-vacancy in crystallographic [111] direction; and trigonal symmetry with point group [13].

For the creation of diamond NV centers, it is necessary to create vacancies inside diamond lattice by two methods: the first one is radiating with ions, electrons or neutrons to nitrogen-rich diamond (^{14}N) type Ib; the second one is through the implantation of nitrogen (both ^{14}N and ^{15}N) inside a pure diamond type IIa which creates simultaneously vacancies in the crystal lattice. Upon creation of the vacancies, it is necessary to perform an annealing process of temperatures around 550°C to 850°C (oxygen atmosphere free) producing the vacancies migration. After this process the NV centers are created [15-17].

3. Charged-states of NV center

Atomic structure of NV center in diamond consist of a carbon vacancy and an impurity of nitrogen which captures this vacancy in order to create the center, furthermore, exhibit two electronic configurations: the neutral charged-state (NV^0) and negatively charged-state (NV^-) [1,13,18].

In the NV^0 center, the nitrogen impurity has five valence electrons (being in group V of the periodic table). Three of them are shared with the three closer atoms of carbon and the other two are located in the direction of the vacancy. Thus, in the periphery of the vacancy, there exist three unsatisfied bonds, one for each of the surrounding carbons (see Fig. 1).

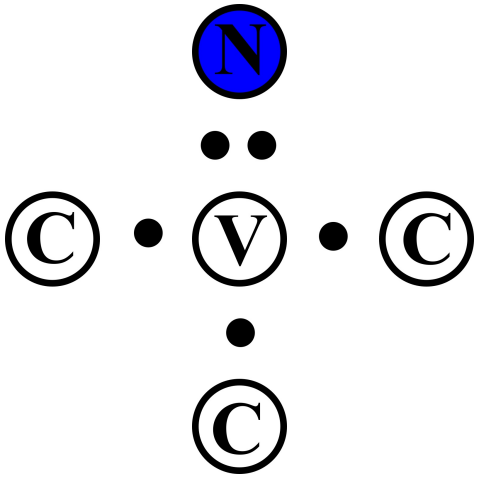

FIGURE 1. Schematic representation in two dimensions of the atomic configuration inside the NV^0 center (where the marked circles with a C simulate the crystalline lattice), in which it can be observed that a carbon atom has been substituted for a nitrogen atom (in color blue), which captures a vacancy (marked as V) that remains with five electrons (black dots) on its direction.

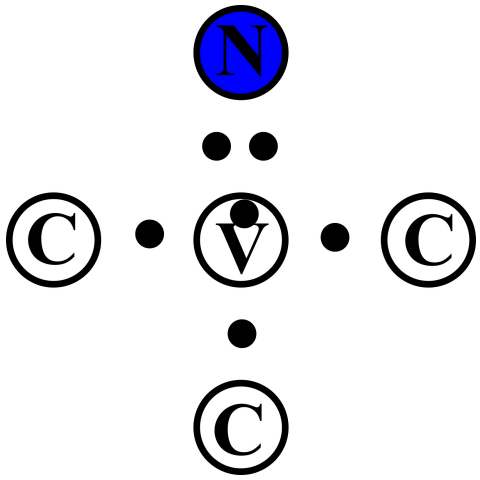

FIGURE 2. Schematic representation in two dimensions of the atomic configuration inside the NV^- center (where the marked circles with a C simulate the crystalline lattice), in which it can be observed that a carbon atom has been substituted for a nitrogen atom (in color blue) which captures a vacancy (marked as V) that remains with five electrons (black dots) on its direction and a sixth electron positioned at the center of the vacancy.

The atomic configuration of NV^- center is the same as the NV^0 center but with the only difference that it has six electrons (see Fig. 2).

4. Electronic configurations

4.1. NV^0 center configuration

As shown in Fig. 1, the nitrogen directs its full orbital towards the vacancy as well as the three surrounding carbons

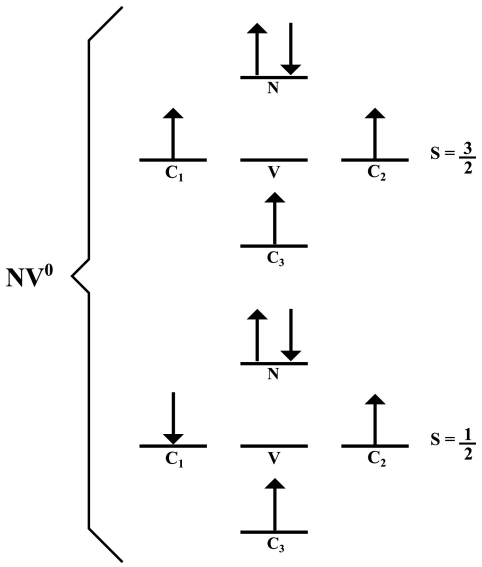

FIGURE 3. Schematic representation of the electron-spin configuration of NV^0 center, in which it is observed the possible values for the total spin S (indicated with black arrows). The lines represent the atoms of nitrogen (N), surrounding carbons (C_1, C_2, and C_3) and the vacancy (V).

their semi-full orbitals point towards it. Therefore, the total spin state (S) can be only 3/2 or 1/2 since the $S = 5/2$ state is not possible because it would be necessary for nitrogen electrons –which point towards the vacancy– to not be paired (see Fig. 3).

4.2. NV^- center configuration

As shown in Fig. 2, the nitrogen directs its full orbital toward the vacancy, the unsatisfied bonds of the surrounding carbons are oriented towards the vacancy, and probably the sixth electron is pushed towards some of the surrounding carbons by effect of the two electrons of the full orbital of the nitrogen; which would very likely result in the paring of the sixth electron with some of the carbons with unsatisfied bonds. Thus, the system could have $S = 2$, $S = 1$ or $S = 0$ states (see Fig. 4).

5. Spin configurations

5.1. NV^0 center

In the case of $S = 1/2$, there are two doublets: one of them being the groud-state with $m_s = \pm 1/2$ and the other one being the excited state as shown in Fig. 5.

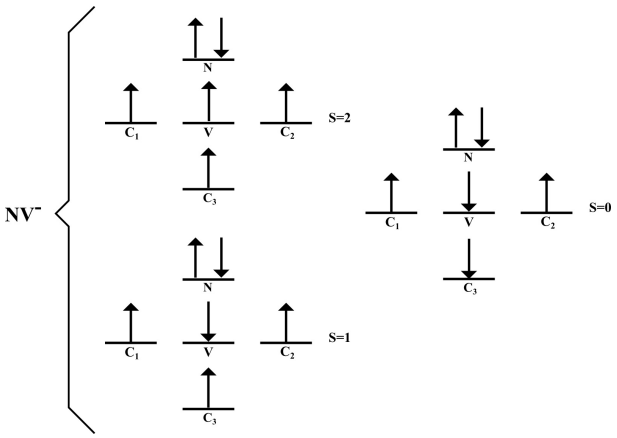

FIGURE 4. Schematic representation of the electron-spin configuration of NV^- center, in which it is observed the possible values for the total spin S (indicated with black arrows). The lines represent the nitrogen atoms (N), surrounding carbons (C_1, C_2, and C_3) and the vacancy (V).

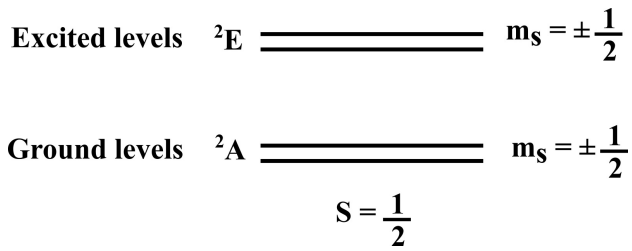

FIGURE 5. Schematic representation of the spin-level structure of a NV^0 center in which the possible $S = 1/2$ spin configuration is observed.

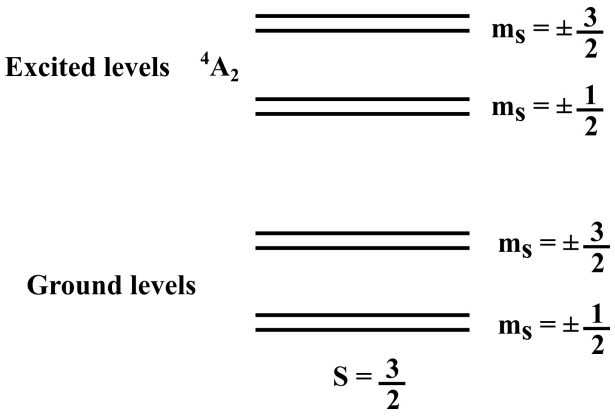

FIGURE 6. Schematic representation of the spin-level structure of a NV^0 center in which the possible $S = 3/2$ spin configuration is observed.

For the case of the $S = 3/2$ state, there are two multiplets: one excited and the other is the ground-state. These are made up of two doublets with $m_s = \pm 1/2$ and $m_s = \pm 3/2$, respectively, as shown in Fig. 6.

5.2. NV^- center

In the case of $S = 2$, there are two multiplets: one excited and the other is the ground-state. These are made up of two doublets ($m_s = \pm 2$ and $m_s = \pm 1$) and one singlet ($m_s = 0$) as shown in Fig. 7.

Similarly, in the case of $S = 1$, there are two triplets: one excited and the other the ground-state. These are made up of a doublet with $m_s = \pm 1$ and one singlet with $m_s = 0$ as shown in Fig. 8. Finally, for the case $S = 0$, there are two singlets: one excited and the other the ground-state; both with $m_s = 0$ as shown in Fig. 9.

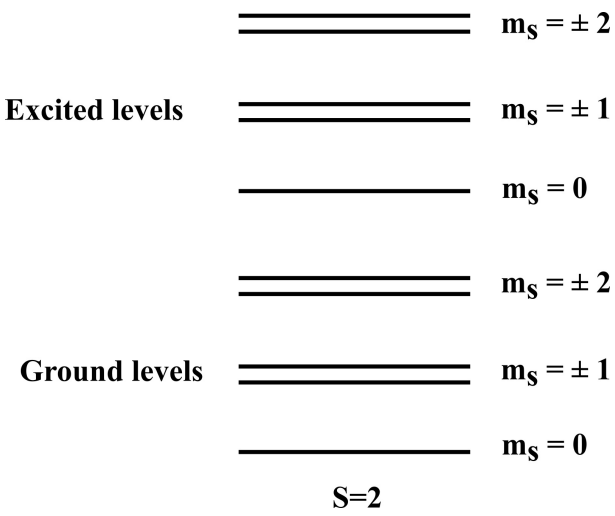

FIGURE 7. Schematic representation of the spin-level structure of a NV^- center, in which the possible $S = 2$ spin configuration is observed.

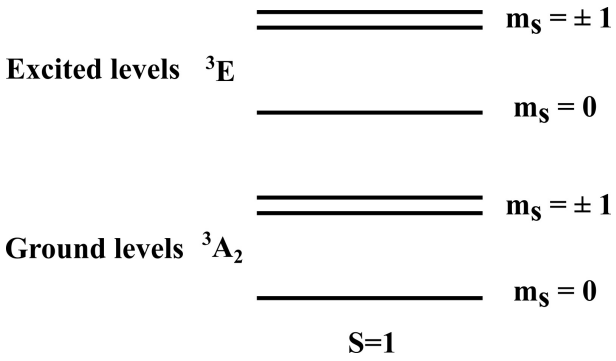

FIGURE 8. Schematic representation of the spin-level structure of a NV^- center in which the possible $S = 1$ spin configuration is observed.

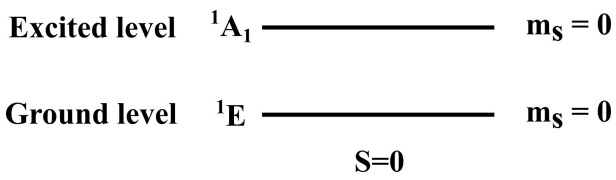

FIGURE 9. Schematic representation of the spin-level structure of a NV^- center in which the possible $S = 0$ spin configuration is observed.

6. Experimental characterization

Experimentally, the NV centers in diamond are characterized by Electron Paramagnetic Resonance (EPR) or Optically Detected Magnetic Resonance (ODMR) techniques and the fluorescence signal emitted when an excited state is relaxed to a base state.

In the NV^0 center, it has been detected a Zero Phonon Line (ZPL) at 2.156 eV (575 nm), which it is associated with a radiative transition ($\Delta m_s = 0$, due to the selection rules present in the system) between the ground (2E) and excited (2A) spin doublets of the $S = 1/2$ state. So far, in the spin-levels ^{2}E and ^{2}A a signal has not been detected using EPR; this is believed to be due to dynamic distortion caused by the Jahn-Teller effect, which causes the EPR lines to widen, preventing its detection [19,20]. In an experiment [20], a paramagnetic resonance using continuous optical illumination in the $S = 3/2$ state was observed, which leads to conclude that it is an spin excited level ($^4A_2$) of the NV^0 center. The $^4A_2$ level consists of a multiplet of two doublets, one of them with $m_s = \pm 3/2$ spin-levels and the other with $m_s = \pm 1/2$ spin-levels (see Fig. 10); between the doublets of the multiplet, there exists a resonance at ~ 1.685 GHz [20]. In conclusion, the ^{2}E and ^{2}A doublets are caused by a $S = 1/2$ state and the $^4A_2$ multiplet is caused by a $S = 3/2$ state. On the other hand, the change between the $S = 1/2$ and $S = 3/2$ states is a result of a non-radiative transition (in this case the mechanism is not spin-conserving, $\Delta m_s \neq 0$). This was demonstrated using the experiment described above and this stems from the fact that the system has to be polarized in the case of the $m_s = \pm 1/2$ spin-levels of the ^{2}A excited levels making that the $m_s = \pm = 1/2$ and $m_s = \pm 3/2$ spin-levels of the $^4A_2$ state populate with greater and lesser probability, respectively (see Fig. 10) [20,21].

In the NV^- center, there exists a radiative transition with spin conservation due to the selection rules present in the system ($\Delta m_s = 0$), from ground spin triplet ($^3A_2$) to excited spin triplet (^{3}E) of the $S = 1$ state. This transition presents a ZPL at 1.945 eV (637 nm) (see Fig. 11) and the spin triplet was demonstrated via ODMR study [22,23] in which was observed a resonance signal at ~ 2.88 GHz between the spin-levels $m_s = 0$ and $m_s = \pm 1$ of spin-level $^3A_2$ [13,24,25]. Furthermore, a non-radiative transition ($\Delta m_s \neq 0$) from the ^{3}E triplet to a spin excited singlet ($^1A_1$) of S=0 state occurs, and then a radiative transition between $^1A_1$ singlet and the spin ground singlet (^{1}E) of $S = 0$ state is observed. That transition was confirmed by observation of an infrared ZPL at 1.185 eV (1046 nm) [26,27]. Finally, a non-radiative transition from the ^{1}E singlet to the $^3A_2$ triplet occurs (see Fig. 11) [26-29]. The transitions between $S = 1$ and $S = 0$ states are non-radiative because they are not spin-conserving. In addition, there is a competition between different non-radiative path of spin-levels of the $S = 1$ state triplets and the $S = 0$ state singlets, that is depicted in Fig. 11. The most likely path between the ^{3}E to the $^1A_1$ is from $m_s = \pm 1$ to $m_s = 0$, respectively and similarly, the transition between the ^{1}E to the $^3A_2$ is from $m_s = 0$ to $m_s = 0$, respectively (see Fig. 11 red wavy arrows). The latter allows the system to be polarized [26-29].

The NV^0 and NV^- centers are promising candidates for solid-state qubits because both centers have characteristics that make them utilizable. In the case of NV^0, it is possible by using a $^4A_2$ excited level since it presents two doublets which can be used as qubit states. Other promising choice would be to use the transition between the ground $m_s = \pm 1/2$ of ^{2}E level and excited $m_s = \pm 1/2$ of ^{2}A level doublets via optical pumping at 2.156 eV following the remotion of the optical excitation, causing the system to decay from the $m_s = \pm 1/2$ ^{2}A level to the $m_s = \pm 1/2$ ^{2}E level. However, there exists a problem with this option because the state loses coherence because of the Jahn-Teller dynamic effect [19,20]. On the other hand, in the case of a NV^- center the process can begin with the $m_s = 0$ $^3A_2$ ground level ($S = 1$) by using optical pumping cycles, manipulated via microwave fields and optical excitations. Measurements can be performed thanks to the fluorescence signal emitted by the decay between the excited and ground spin levels following the selection rules of the radiative transitions.

7. Theoretical characterization

The spin-orbital interaction, spin-spin interaction with electric and strain fields (see Eqs. (6), (8), (13), and (17)) are all Hamiltonians in terms of the Irreducible Representations (IRs) by, using Group Theory and are discussed in Ref. [30].

The electronic Hamiltonian of the NV^- center (Eq. (1)) –corresponding to the ground electronic state– with an adiabatic approximation and considering the nuclei of the crystal to be fixed at their equilibrium coordinates is shown in [31]. The interaction Hamiltonians of the center with electric (Stark shift), magnetic (Zeeman effect), and strain fields of Eq. (16) are shown in Ref. [32].

In Ref. [5] the ground state fine and hyperfine structures for both nitrogen isotopes can be described by the canonical spin-Hamiltonian of trigonal defects given by Eq. (1) and the potential of Eq. (2) describes the influence of static electric, magnetic, and strain fields on the NV^- ground state. Also, it is shown the effective Hamiltonian and potential that describes the influence of static electric, magnetic, and strain fields for excited state 3E to low-temperature and room-temperature (see Eqs. (3)-(6)).

7.1. Steady-state (Conservative model)

In the present paper, the Hamiltonian of NV center, $\hat{H}_{sys}$ which only describes the internal state defect without external perturbation, is composed of the spin-spin interaction, $\hat{H}_{S-S}$, the spin-orbital interaction (fine structure), $\hat{H}_{L-S}$, and the electron-nuclear spin coupling (hyperfine structure) $\hat{H}_{I-S}$. Notice that the nuclear-nuclear spin coupling has not been considered because, in the case of a nitrogen ^{15} isotope, the system does not have electric quadrupole moment. Consequently,

$$\hat{H}_{sys} = \hat{H}_{S-S} + \hat{H}_{L-S} + \hat{H}_{I-S}, \tag{1}$$

$$\hat{H}_{S-S} = \sum_i \sum_j \frac{\mu_0 \gamma_e^2}{4\pi r^3}[\overrightarrow{S}_i \cdot \overrightarrow{S}_j - 3(\overrightarrow{S}_i \cdot \overrightarrow{n}_{ij})(\overrightarrow{n}_{ij} \cdot \overrightarrow{S}_j)],$$

$$\overrightarrow{S}_i = S_{i_x}\hat{\mathbf{i}} + S_{i_y}\hat{\mathbf{j}} + S_{i_z}\hat{\boldsymbol{k}}, \tag{2}$$

$$\hat{H}_{L-S} = -\sum_i \gamma_e \overrightarrow{B} \cdot \overrightarrow{S}_i = -\sum_i \frac{g_s \mu_B}{\hbar m_e e c^2 r} \overrightarrow{L}_i \cdot \overrightarrow{S}_i$$

$$= -\sum \frac{\gamma_e}{m_e e c^2 r} \overrightarrow{L}_i \cdot \overrightarrow{S}_i, \tag{3}$$

$$\hat{H}_{I-S} = \sum_i \sum_j \frac{\mu_0 \gamma_e \gamma_n}{4\pi r^3}$$

$$\times \left[\overrightarrow{I}_i \cdot \overrightarrow{S}_j - 3(\overrightarrow{I}_i \cdot \overrightarrow{n}_{ij})(\overrightarrow{n}_{ij} \cdot \overrightarrow{S}_j) \right],$$

$$\overrightarrow{S}_j = S_{j_x}\hat{\mathbf{i}} + S_{j_y}\hat{\mathbf{j}} + S_{j_z}\hat{\boldsymbol{k}},$$

$$\overrightarrow{I}_i = I_{i_x}\hat{\mathbf{i}} + I_{i_y}\hat{\mathbf{j}} + I_{i_z}\hat{\boldsymbol{k}}, \tag{4}$$

where the index i, and j represent the NV center electrons, μ_0 represents the magnetic constant (vacuum permeability), γ_e and γ_n are the electron and nuclear gyromagnetic constants, respectively, S indicates the magnitude of the total electron-spin of the system $\overrightarrow{S}_i$ and $\overrightarrow{I}_i$ represent the electron and nuclear spin vectors, respectively, m_e is the electron mass value, c is the speed light constant in vacuum, r symbolizes the distance between interacting electrons, and $\overrightarrow{n}_{ij}$ stands for a unit vector which shows the interacting direction between electron-spins.

On the other hand, the steady-state solution (conservative) will be,

$$\hat{H}_{sys}|\Psi_{NV}\rangle = E|\Psi_{NV}\rangle, \tag{5}$$

using the second quantization formalism, the form of a NV^0 center wave can be written as follows

$$|\Psi_{\mathrm{NV}}\rangle = A\sum_i C_i(r,\sigma,t)|\Psi^{(0)}_{\mathrm{NV}^0}(r,\sigma,t)\rangle, \tag{6}$$

where the index i indicates the center electrons, (r,σ,t) represent the spatial coordinates, electron-spin and time, respectively. A symbolizes a normalization constant, C_i is a proportional constant, and $|\Psi^{(0)}_{NV^0}(r,\sigma,t)\rangle$ denotes the non-interacting wave function, which is composed of products of single-electron functions, namely,

$$|\Psi^{(0)}_{\mathrm{NV}^0}(r,\sigma,t)\rangle = \frac{1}{\sqrt{4!}}\sum_p (-1)^{\mathrm{NV}}|\Phi^{(0)}_{C_1}(\vec{r}_1,\sigma_1,t)\rangle$$

$$\times |\Phi^{(0)}_{C_2}(\vec{r}_2,\sigma_2,t)\rangle|\Phi^{(0)}_{C_3}(\vec{r}_3,\sigma_3,t)\rangle$$

$$\times |\Phi^{(0)}_{V_o}(\vec{r}_4,\sigma_4,t)\rangle. \tag{7}$$

Similarly, it is obtained the non-interacting wave function of the NV^- center,

$$|\Psi^{(0)}_{\mathrm{NV}^-}(r,\sigma,t)\rangle = \frac{1}{\sqrt{4!}}\sum_p (-1)^{NP}|\Phi^{(0)}_{C_1}(\vec{r}_1,\sigma_1,t)\rangle$$

$$\times |\Phi^{(0)}_{C_2}(\vec{r}_2,\sigma_2,t)\rangle|\Phi^{(0)}_{C_3}(\vec{r}_3,\sigma_3,t)\rangle$$

$$\times |\Phi^{(0)}_{V_1}(\vec{r}_4,\sigma_4,t)\rangle, \tag{8}$$

where summation is done over all different possible p permutations and N_p represents the permutation index, C_1, C_2, C_3 represent the three unbonded carbons, and V represents an electron in the vacancy (see Fig. 2). Notice that the subindex on V in the function $\Phi^{(0)}_{V_i}$, represent an empty vacancy (NV^0 center) or an occupied vacancy for the values $i=0$ or $i=1$, respectively.

Now, if the wave functions of NV^0 and NV^- centers are projected on the symmetrical occupation-number basis $\{|n\rangle\}$ in a Folk space, it leads to:

$$|\Psi'_{\mathrm{NV}^0}\rangle = \sum_n \langle n|\Psi_{\mathrm{NV}^0}(\vec{r},\sigma,t)\rangle$$

$$= \sum_n \Psi'_{\mathrm{NV}^0{}_n}(\vec{r},\sigma,t)|n\rangle, \tag{9}$$

$$|\Psi'_{\mathrm{NV}^-}\rangle = \sum_n \langle n|\Psi_{\mathrm{NV}^-}(\vec{r},\sigma,t)\rangle$$

$$= \sum_n \Psi'_{\mathrm{NV}^-{}_n}(\vec{r},\sigma,t)|n\rangle, \tag{10}$$

and defining $\hat{\alpha}_V^\dagger$, $\hat{\alpha}_V$ as, creation and annihilation operators, respectively, which acts only on the vacancy state, ***i.e.***,

$$\hat{\alpha}_V^\dagger = \sum_n \sqrt{n_V}|n_{C_1}, n_{C_2}, n_{C_3}, n_V - 1\rangle \times \langle n_{C_1}, n_{C_2}, n_{C_3}, n_V|, \quad (11)$$

$$\hat{\alpha}_V = \sum_n \sqrt{n_V + 1}|n_{C_1}, n_{C_2}, n_{C_3}, n_V + 1\rangle \times \langle n_{C_1}, n_{C_2}, n_{C_3}, n_V|. \quad (12)$$

When the operators given by Eqs. (11) and (12) are applied onto the wave functions of Eqs. (9) and (10), the result is

$$\hat{\alpha}_V^\dagger|\Psi'_{\mathrm{NV}^0}\rangle = |\Psi'_{\mathrm{NV}^-}\rangle; \quad \hat{\alpha}_V\hat{\alpha}_V^\dagger|\Psi'_{\mathrm{NV}^0}\rangle = |\Psi'_{\mathrm{NV}^0}\rangle, \quad (13)$$

$$\hat{\alpha}_V|\Psi'_{\mathrm{NV}^-}\rangle = |\Psi'_{\mathrm{NV}^0}\rangle; \quad \hat{\alpha}_V^\dagger\hat{\alpha}_V|\Psi'_{\mathrm{NV}^-}\rangle = |\Psi'_{\mathrm{NV}^-}\rangle. \quad (14)$$

Thus, from (13) and (14), it can be concluded that $[\hat{\alpha}_V^\dagger, \hat{\alpha}_V] = 1$ for both.

Since the previous wave functions, (7) and (8), depend on the spin σ, then they can be rewritten as the product of their orbital wave function $|\Phi(\vec{r}, t)\rangle$ and its spinorial function $|X(\sigma, t)\rangle$, that is:

$$|\Psi^{(0)}_{\mathrm{NV}^0}(\vec{r}, \sigma, t)\rangle = |\Phi_{\mathrm{NV}^0}(\vec{r}, t)\rangle|X_{\mathrm{NV}^0}(\sigma, t)\rangle, \quad (15)$$

$$|\Psi^{(0)}_{\mathrm{NV}^-}(\vec{r}, \sigma, t)\rangle = |\Phi_{\mathrm{NV}^-}(\vec{r}, t)\rangle|X_{\mathrm{NV}^-}(\sigma, t)\rangle. \quad (16)$$

Therefore, the form of the spinorial functions of the NV^0 and NV^- centers can be obtained from

$$|X_{\mathrm{NV}^0}(\sigma, t)\rangle = \frac{1}{\sqrt{3!}}\sum_p (-1)^{Np}|\chi^{(0)}_{C_1}(\sigma_1, t)\rangle \times |\chi^{(0)}_{C_2}(\sigma_2, t)\rangle|\chi^{(0)}_{C_3}(\sigma_3, t)\rangle, \quad (17)$$

$$|X_{\mathrm{NV}^-}(\sigma, t)\rangle = \frac{1}{\sqrt{4!}}\sum_p (-1)^{Np}|\chi^{(0)}_{C_1}(\sigma_1, t)\rangle|\chi^{(0)}_{C_2}(\sigma_2, t)\rangle \times |\chi^{(0)}_{C_3}(\sigma_3, t)\rangle|\chi^{(0)}_{V}(\sigma_4, t)\rangle, \quad (18)$$

where summation is performed over all different possible permutations p of the system, C_1, C_2, C_3 represent the three unbonded carbons, and V represents an electron to place in the vacancy (see Fig. 2). As the negatively charged-state center NV^- is the best candidate to implement as a solid-state qubit based on the DiVenzo Criteria [33], it will be the focus of the present study. The electrons of NV^- center that are involved in the processes of the radiative and non-radiative transitions are the three of the carbons that have unsatisfied bonds and an extra that is transferred by some close donor impurity into the vacancy. Therefore, there are four electrons participating in the different $S = 0$ and $S = 1$ spin states; $S = 2$ will be omitted because there is not experimental evidence for this spin configuration. Accordingly, the possible forms of the spinorial function of Eq. (18) for the two different spin states in ground state are

- $S = 0, \quad m_s = 0$

$$|X_{\mathrm{NV}^-}(\sigma, t)\rangle = \frac{1}{2}(\alpha_{C_1}\alpha_{C_2}\beta_{C_3}\beta_V - \alpha_{C_1}\beta_{C_2}\beta_{C_3}\alpha_V + \beta_{C_1}\beta_{C_2}\alpha_{C_3}\alpha_V - \beta_{C_1}\alpha_{C_2}\alpha_{C_3}\beta_V) \quad (19)$$

- $S = 1, \quad m_s = 1$

$$|X_{\mathrm{NV}^-}(\sigma, t)\rangle = \alpha_{C_1}\alpha_{C_2}\alpha_{C_3}\alpha_V \quad (20)$$

- $S = 1, \quad m_s = 0$

$$|X_{\mathrm{NV}^-}(\sigma, t)\rangle = \frac{1}{2}(\alpha_{C_1}\alpha_{C_2}\beta_{C_3}\beta_V + \alpha_{C_1}\beta_{C_2}\beta_{C_3}\alpha_V + \beta_{C_1}\beta_{C_2}\alpha_{C_3}\alpha_V + \beta_{C_1}\alpha_{C_2}\alpha_{C_3}\beta_V) \quad (21)$$

- $S = 1, \quad m_s = 1$

$$|X_{\mathrm{NV}^-}(\sigma, t)\rangle = \gamma_{C_1}\gamma_{C_2}\gamma_{C_3}\gamma_V \quad (22)$$

where C_1, C_2, C_3 represent the three unbonded carbons, and V represents an electron to place in the vacancy (see Fig. 2). Furthermore, the α_k, β_k, and γ_k states are characterized by the index k, which can take the values of C_1, C_2, C_3, or V and are defined as

$$\alpha \equiv \begin{pmatrix} 1 & 0 & 0 \\ 0 & 0 & 0 \\ 0 & 0 & 0 \end{pmatrix} \quad \beta \equiv \begin{pmatrix} 0 & 0 & 0 \\ 1 & 0 & 0 \\ 0 & 0 & 0 \end{pmatrix}$$

$$\gamma \equiv \begin{pmatrix} 0 & 0 & 0 \\ 0 & 0 & 0 \\ 1 & 0 & 0 \end{pmatrix}. \quad (23)$$

Well, if the $|X_{\mathrm{NV}^-}(\sigma, t)\rangle$ spinorial function is projected on the symmetrical occupation-number basis $\{|n\rangle\}$ in a Folk space, it leads to

$$|X'_{\mathrm{NV}^-}(\sigma, t)\rangle = \sum_n \langle n|\chi_{\mathrm{NV}^-}(\sigma, t)\rangle = \sum_n \langle \chi'_{\mathrm{NV}^-_n}(\sigma, t)|n\rangle, \quad (24)$$

where $X'_{\mathrm{NV}^-_n}(\sigma, t)$ represents a single-electron spinor on n state of the $|X'_{\mathrm{NV}^-}(\sigma, t)\rangle$ spinorial function. Now, if $t = t_0$ is fixed, it leads to steady-states as it follows

$$|X'_{\mathrm{NV}^-}(\sigma, t_0)\rangle = \sum_{n=1}^{8} \chi'_{\mathrm{NV}^-_n}(\sigma, t_0)|n\rangle \quad (25)$$

where the eight $|n\rangle$ states (four ground and four excited) are represented by

- $S = 0$

$|1\rangle$ is the $m_s = 0$ ground state and $|2\rangle$ is the $m_s = 0$ excited state (26)

- $S = 1$

  $|3\rangle$ is the $m_s = 0$ ground state and $|4\rangle$ is the $m_s = 0$ excited state;

  $|5\rangle$ is the $m_s = -1$ ground state and $|6\rangle$ is the $m_s = -1$ excited state;

  $|7\rangle$ is the $m_s = 1$ ground state and $|8\rangle$ is the $m_s = 1$ excited state (27)

The expressions of Eqs. (26) and (27) have been depicted in the Figs. 8 and 9 of Sec. 5.2 according to their spin-level structure.

7.2. Dynamic-state (Non-conservative model)

The dynamic Hamiltonian $\hat{H}_{dyn}$, is composed of the NV center and electromagnetic field Hamiltonians denoted by $\hat{H}_{sys}$ and $\hat{H}_{int}$, respectively (see Eqs. (1)-(4)); the resulting Hamiltonian has the following form:

$$\hat{H}_{dyn} = \hat{H}_{sys} + \hat{H}_{int}, \tag{28}$$

where

$$\hat{H}_{int} = \sum_{\lambda} \hbar\omega_{\lambda} \left(\hat{a}^{\dagger}_{\lambda} \hat{a}_{\lambda} + \frac{1}{2} \right). \tag{29}$$

Therefore, the dynamic-state solution (conservative) will be,

$$i\hbar \frac{\partial}{\partial t} |\Psi_{\text{NV}}\rangle = \hat{H}_{dyn} |\Psi_{\text{NV}}\rangle. \tag{30}$$

Well, substituting (10) into (30), it is possible to obtain an expression for the NV^- center, namely, center

$$i\hbar \frac{\partial}{\partial t} |\Psi'_{\text{NV}^-}\rangle = \hat{H}_{dyn} \sum_{n} \Psi'_{\text{NV}^- n}(\vec{r}, \sigma, t) |n\rangle. \tag{31}$$

The creation and annihilation operators for the NV^- center between its electron-spin states, from (31), acquire the form

$$\hat{a}^{\dagger}_{S,m_s} = \sqrt{n_{S,m_s}} |n_{S,m_s} + 1\rangle\langle n_{S,m_s}|, \tag{32}$$

$$\hat{a}_{S,m_s} = \sqrt{n_{S,m_s} + 1} |n_{S,m_s} - 1\rangle\langle n_{S,m_s}|, \tag{33}$$

where the $|n_{S,m_s}\rangle$ are identified by its spin value S and spin momentum on z-direction m_s. Thus, the transitions between the ground-states and excited-states (see Fig. 11) can be obtained from

$$T_{n \to n*} = \frac{2\pi}{\hbar} |\langle n^* | \hat{H}_{\text{int}} | n \rangle|^2 \rho(E_{n^*}),$$

Fermi's Golden Rule (34)

where $|\langle n^*|\hat{H}_{\text{int}}|n\rangle$ is the matrix element of the interaction $\hat{H}_{int}$ between the final n^* and initial n states and $\rho(E_{n^*})$ is the density of states at the energy of the final states. The density of states for both centers NV is discrete and is defined as

$$\rho(E) = \sum_{i} \delta(E - E_i), \tag{35}$$

where i is the set of spin states for each different charged-state of NV centers. If the same energy interval is chosen, therefore the number of states of a NV^0 center is greater than for NV^-, meaning that

- NV^0 center has two different total spin states, and these are $S = 1/2$ and $S = 3/2$.
- NV^- center has two different total spin states, and these are $S = 1$ and $S = 0$.

Based on the above and reviewing the spin-level structures for the charged-state of each center (see Fig. 5-6 for NV^0 and Fig. 8-9 for NV^-), it is concluded that the density of states of NV^0 $\rho(E)$ is greater than the one for NV^-, $\rho'(E)$. The density of states on the photochromism phenomenon changes from $\rho(E)$ to $\rho'(E)$ and viceversa. From this fact, a total density of states $\rho_T(E)$ can be defined as

$$\rho_T(E) = a\rho(E) + b\rho'(E), \tag{36}$$

which, when $a = 0$ and $b = 1$, represents the density of states of NV^-. In turn, if $a = 1$ and $b = 0$, it represents the density of states of NV^0. Accordingly,

$$\begin{aligned} \hat{a}_{S,m_S} |n_{S,m_S}\rangle &= \sqrt{n_{S,m_S} + 1} |n_{S,m_S} - 1, n_{S,m^*_S}\rangle, \\ \hat{a}^{\dagger}_{S,m^*_S} \hat{a}_{S,m_S} |n_{S,m_S}\rangle &= \sqrt{n_{S,m_S} (\hat{a}_{S,m_S} + 1)} \\ &\quad \times |n_{S,m_S} - 1, n_{S,m^*_S} + 1\rangle, \\ \langle n^* | \hat{H}_{\text{int}} | n \rangle &\propto \langle n^*_{S,m_S} | \hat{a}^{\dagger}_{S,m_S} \hat{a}_{S,m_S} | n_{S,m_S} \rangle. \end{aligned} \tag{37}$$

Therefore, $\hat{a}^{\dagger}_{S,m^*_S}$ and $\hat{a}_{S,m_S}$ work on different states, ground or excited, but always following the selection rule dictated by $\Delta m_s = 0$. This is, if $\hat{a}_{S,m_S}$ annihilates an electron on the $S = 1$, $m_s = 0$ ground state, $\hat{a}^{\dagger}_{S,m^*_S}$ creates an electron on the $S = 1$, $m^*_s = 0$ excited state; in other words, it is a transition caused by the electromagnetic interaction.

8. Discussion of results

On the previous section, the different models, assumptions, and approximations reported in the literature for NV centers in diamond. By comparison with the present model, the main differences with respect of the models above are the use of the second quantization formalism and the photochromism phenomenon.

In this section, the most important results obtained for the characterization of the NV center internal state will be shown using the second quantization formalism, including the photochromism effect. First, the schematic representations of the two different NV center electronic configurations, neutral

and negative charged-states, was designed in order to clarify how the different possible configurations of each electron-spin modify the system total spin S. The fact that diamond is the host lattice of the NV defect plays a very important role because if it was not for the diamond energy potential, the NV center would not exist. It must also be noted that the defect behaves as an internal system within the diamond matrix, since the spin-levels are in the middle, above the valence band which is populated and below the conduction band which is empty, both bands belong to the diamond; in other words, the electrons of the diamond lattice do not play a role within the dynamics of the NV center. Considering the previous assertions, the Hamiltonian modeling of the system internal state, $\hat{H}_{sys}$ (see Eqs. (1)-(4)) is justified. Therefore, it was applied the second quantization formalism on the $\hat{H}_{sys}$ model (see Eqs. (9) and (10)). From Eq. (10), the ground-levels for different spin-states in the steady state of the NV^- center were determined (see Eqs. (19)-(22)), which are also compatible with those shown in Figs. 8 and 9. Thus, it can be stated that this model reproduces the spin-levels structure of the system.

On the other hand, the NV center exhibits a switching charged-state process called photochromism [1]. There are two different ways to describe this phenomenon:

- The one described in Ref. [1] presents the hypothesis that the switch from NV^0 to NV^- state is photoinduced. This process would be possible due to the ionization of nitrogen donors present in the surroundings of NV defect.

- The other hypothesis suggested is by means of the existence of a weak interaction between NV^0 and NV^- centers, which are created in almost the same proportion in diamond during the production process. This interaction is due to the interchange of vacancy-electron from NV^- to NV^0, resulting in a switching charged-state steady-process. Therefore, the creation and annihilation operators of Eqs. (11) and (12), respectively, are useful to describe the photochromism since they switch the defect from NV^0 to NV^- center and vice versa.

Finally, from $\hat{H}_{dyn}$ (see Eq. (28)) it was possible to obtain the transitions between ground- and excited-states (see Fig. 11), which describe the system dynamics of the NV^- center. This description is really important because it is necessary for the design of solid-state qubits. A qubit is the quantum counterpart of the classical bit, which means it is the minimal unit of information in Quantum Informatics and essential difference of a qubit and a bit relies on the fact that the qubit can present a superposition between two states, whereas the classical counterpart can only represent one state at a time. Therefore, the spin-levels $m_s = 0$ and $m_s = -1$, in ground-state $S = 1$ of the NV^- center (see Fig. 8) can represent such states of the qubit; that is,

$$|\Psi\rangle = \alpha|0\rangle + \beta|-1\rangle, \tag{38}$$

where α and β are complex coefficients that satisfy $|\alpha|^2 + |\beta|^2 = 1$.

To make use of the NV^- center as a qubit, it will be necessary to use the spin-levels of its different states, ground and excited. For example, by taking advantage of the photoluminescent response that the system undergoes, when it passes from an excited level to a ground level, the system configuration can be found, meaning that the system is read-out. On the other hand, applying a magnetic field tuned to a suitable resonance frequency, the manipulation of the electron population of ground and excited states can be achieved. Finally, due to the existence of the two different spin configuration, $S = 1$ and $S = 0$, it is possible to initialize the system in a specific spin-level.

Now that the procedure has already been proposed, it is necessary to know what spin-levels are more convenient to represent the two qubit states. There are two possibilities to represent these qubit states. The first one would be to use the ground-state levels, $m_s = 0$ and $m_s = -1$ –the most advisable for energy efficiency– which would represent the qubit states. To avoid the mixing between the spin levels, a magnetic field would need to be applied to make use of the Zeeman effect, splitting the levels and, consequently, decreasing the mixing probability. The other possibility is to use the photochromism phenomenon by manipulating the configuration of two different NV centers, one with $S = 1$ and the other one with $S = 0$ as qubit states. In this case, the initialization can be represented by means of one of the two configurations of total spin S; the manipulation would be through electron population distribution in different configurations of spin using magnetic and electromagnetic fields. Finally, the measurement would be performed using the ZPL, which represents every spin configuration. This possibility could be deeply studied in another future paper.

9. Conclusions

Based on the above, the NV^- center is promising because of its characteristics. It is concluded that a possible candidate for solid-state qubit requires the following features:

- The host lattice of the defect should show a low coupling between the system electrons and the lattice phonons (high Debye temperature) in order to work at room temperature. In addition, the lattice symmetry may be C_{3v} with the purpose to obtain a triplet-spin system.

- To have radiative transitions between different spin levels and in the case that they are degenerate, it must be possible to split them by external means (*i.e.*, a magnetic/electric field or stress application) in order to avoid mixed states. However, the radiative transitions are not necessarily the only way, since there might be alternatives on the condition that the read-out signal presents few difficulties during the measurement.

- The system must allow to be initialized, manipulated, and measured via external means.

Acknowledgments

This work was supported by CONACyT.

Conflict of Interest Statement

The authors declare that the research was conducted in the absence of any commercial or financial relationship that could be construed as a potential conflict of interest.

1. T. Gaebel et al., Photochromism in signle nitrogen-vacancy defect in diamond, *Appl. Phys. B* **82** (2006) 243, https://doi.org/10.1007/s00340-005-2056-2.
2. F. Shi et al., Room-Temperature Implementation of the Deutsch-Joszsa Algorithm with a Single Electronic Spin in Diamond, *Phys. Rev. Lett.* **105** (2010) 040504, https://doi.org/10.1103/PhysRevLett.105.040504.
3. S. Hong et al., Nanoscale magnetometry with NV centers in diamond, *MRS Bull.* **38** (2013) 155, https://doi.org/10.1557/mrs.2013.23.
4. J. S. Hodges et al., Timekeeping with electron spin states in diamond, *Phys. Rev. A* **87** (2013) 032118, https://doi.org/10.1103/PhysRevA.87.032118.
5. M. W. Doherty et al., The nitrogen-vacancy colour centre in diamond, *Phys. Rep.* **528** (2013) 1, https://doi.org/10.1016/j.physrep.2013.02.001.
6. D. Kielpinski, C. Monroe, and D. J. Wineland, Architecture for a large-scale ion-trap quantum computer, *Nature* **417** (2002) 709, https://doi.org/10.1038/nature00784.
7. G. GonzÃ¡lez and M. N. Leuenberger, The dynamics of the optically driven Λ transition of the ^{15}N-V^{-} center in diamond, *Nanotechnology* **21** (2010) 274020, https://doi.org/10.1088/0957-4484/21/27/274020.
8. D. Loss and D. P. DiVincenzo, Quantum computation with quantum dots, *Phys. Rev. A* **57** (1998) 120, https://doi.org/10.1103/PhysRevA.57.120.
9. D. G. Cory *et al.*, NMR Based Quantum Information Processing: Achievements and Prospects, *Fortschr. Phys.* **48** (2000) 875, https://doi.org/10.1002/1521-3978(200009)48:9/11⟨875::AID-PROP875⟩3.0.CO;2-V.
10. J. A. Jones, NMR Quantum Computation: A Critical Evaluation, *Fortschr. Phys.* **48** (2000) 909, https://doi.org/10.1002/1521-3978(200009)48:9/11⟨909::AIDPROP909⟩3.0.CO;2-2.
11. C. H. van der Wal et al., Quantum Superposition of Macroscopic Persistent-Current States, *Science* **290** (2000) 773, https://doi.org/10.1126/science.290.5492.773.
12. T. Gaebel *et al.*, Room-temperature coherent coupling of single spins in diamond, *Nat. Phys.* **2** (2006) 408, https://doi.org/10.1038/nphys318.
13. C. Bradac, T. Gaebel, J. R. Rabeau, and A. S. Barnard, in *Nanotechnology in Australia*, edited by D. Kane, A. Micolich, and J. Rabeau (Pan Stanford Publishing, Singapore, 2011), pp. 113-149.
14. G. Balasubramanian et al., Ultralong spin coherence time in isotopically engineered diamond, *Nat. Mater.* **8** (2009) 383, https://doi.org/10.1038/nmat2420.
15. J. Meijer et al., Generation of single color centers by focused nitrogen implantation, *Appl. Phys. Lett.* **87** (2005) 261909, https://doi.org/10.1063/1.2103389.
16. J. R. Rabeau et al., Implantation of labelled single nitrogen vacancy centers in diamond using ^{15}N, *Appl. Phys. Lett.* **88** (2006) 023113, https://doi.org/10.1063/1.2158700.
17. A. V. Tsukanov, NV-centers in diamond. Part I. General information, fabrication technology, and the structure of the spectrum, *Russ. Microelectron.* **41** (2012) 91, https://doi.org/10.1134/S1063739712020084.
18. A. Lenef et al., Electronic structure of the N-V center in diamond: Experiments, *Phys. Rev. B* **53** (1996) 13427, https://doi.org/10.1103/PhysRevB.53.13427.
19. G. Davies, Dynamic Jahn-Teller distortions at trigonal optical centres in diamond, *J. Phys. Condens. Matter* **12** (1979) 2551, https://doi.org/10.1088/0022-3719/12/13/019.
20. S. Felton *et al.*, Electron paramagnetic resonance studies of the neutral nitrogen vacancy in diamond, *Phys. Rev. B* **77** (2008) 081201(R), https://doi.org/10.1103/PhysRevB.77.081201.
21. A. Gali, Theory of the neutral nitrogen-vacancy center in diamond and its application to the realization of a qubit, *Phys. Rev. B* **79** (2009) 235210, https://doi.org/10.1103/PhysRevB.79.235210.
22. P. Neumann et al., Excited-state spectroscopy of single NV defects in diamond using optically detected magnetic resonance, *New J. Phys.* **11** (2009) 013017, https://doi.org/10.1088/1367-2630/11/1/013017.
23. A. Gruber *et al.*, Scanning Confocal Optical Miscroscopy and Magnetic Resonance on Single Defect Centers, *Science* **276** (1997) 2012, https://doi.org/10.1126/science.276.5321.2012.
24. J. H. N. Loubser and J. A. van Wyk, Electron spin resonance in the study of diamond, *Rep. Prog. Phys.* **41** (1978) 1201, https://doi.org/10.1088/0034-4885/41/8/002.
25. L. J. Rogers, S. Armstrong, M. J. Sellars, and N. B. Manson, Infrared emission of the NV centre in diamond: Zeeman and uniaxial stress studies, *New J. Phys.* **10** (2008) 103024, https://doi.org/10.1088/1367-2630/10/10/103024.
26. L. J. Rogers et al., Singlet levels of the NV^{-} centre in diamond, *New J. Phys.* **17** (2015) 013048, https://doi.org/10.1088/1367-2630/17/1/013048.

27. J. R. Weber et al., Quantum computing with defects, *Proc. Natl. Acad. Sci.* **107** (2010) 8513, https://doi.org/10.1073/pnas.1003052107.

28. N. B. Manson, J. P. Harrison, and M. J. Sellars, Nitrogen-vacancy center in diamond: Model of the electronic structure and associated dynamics, *Phys. Rev. B* **74** (2006) 104303, https://doi.org/10.1103/PhysRevB.74.104303.

29. J. R. Maze, Properties of nitrogen-vacancy centers in diamond: the group theoretic approach, *New J. Phys.* **13** (2011) 025025, https://doi.org/10.1088/1367-2630/13/2/025025.

30. M. W. Doherty, N. B. Manson, P. Delaney, and L. C. L. Hollenberg, The negatively charged nitrogen-vacancy centre in diamond: the electronic solution, *New J. Phys.* **13** (2011) 025019, https://doi.org/10.1088/1367-2630/13/2/025019.

31. M. W. Doherty et al., Theory of the ground-state spin of the NV^- center in diamond, *Phys. Rev. B* **85** (2012) 205203, https://doi.org/10.1103/PhysRevB.85.205203.

32. D. P. DiVincenzo, The Physical Implementation of Quantum Computation, Fortsch. *Phys.* **48** (2000) 771, https://doi.org/10.1002/1521-3978(200009)48:9/11⟨771::AIDPROP771⟩3.0.CO;2-E.